Photoacoustics 10 (2018) 31–37

Contents lists available at ScienceDirect

Photoacoustics

journal homepage: www.elsevier.com/locate/pacs

Research article

Assessing nailfold microvascular structure with ultra-wideband raster-scan optoacoustic mesoscopy

J. Aguirre[a,1], B. Hindelang[b,1], A. Bereznhoi[a], U. Darsow[b], F. Lauffer[b], K. Eyerich[b], T. Biedermann[b], V. Ntziachristos[a,*]

[a] Chair of Biological Imaging, Technische Universität München and Institute of Biological and Medical Imaging, Helmholtz Zentrum München, Neuherberg, Germany
[b] Department of Dermatology and Allergy, Technische Universität München, Munich, Germany

ARTICLE INFO

Article history:
Received 17 November 2017
Received in revised form 8 February 2018
Accepted 14 February 2018
Available online 21 February 2018

ABSTRACT

Nailfold capillaroscopy, based on bright-field microscopy, is widely used to diagnose systemic sclerosis (SSc). However it cannot reveal information about venules and arterioles lying deep under the nailfold, nor can it provide detailed data about surface microvasculature when the skin around the nail is thick. These limitations reflect the fact that capillaroscopy is based on microscopy methods whose penetration depth is restricted to about 200 μm. We investigated whether ultra-wideband raster-scan optoacoustic mesoscopy (UWB-RSOM) can resolve small capillaries of the nailfold in healthy volunteers and compared the optoacoustic data to conventional capillaroscopy examinations. We quantified UWB-RSOM-resolved capillary density and capillary diameter as features that relate to SSc biomarkers, and we obtained the first three-dimensional, *in vivo* images of the deeper arterioles and venules. These results establish the potential of UWB-RSOM for analyzing SSc-relevant markers.

1. Introduction

Nailfold capillaroscopy, based on optical microscopy, is an important clinical technique for assessing microvascular structure that can support early diagnosis of systemic sclerosis (SSc), also known as scleroderma [1,2]. It can also help predict whether SSc patients are likely to develop vascular and visceral complications potentially limiting their life expectancy, and it can aid in the differential diagnosis of SSc-related conditions. The technique is widely accepted as a diagnostic tool [3–5], even forming part of the diagnostic criteria of SSc defined by the American College of Rheumatology and the European League Against Rheumatism [6]. However, capillaroscopy does not provide detailed images of nailfold microvasculature under certain conditions, such as when the patient's skin around the nail is thick [7,8]. The penetration depth of optical microscopy is limited to approximately 200 μm because tissue strongly scatters light [9], and penetration is even shallower (few tens of micrometers) for the bright-field microscopy used for capillaroscopy [9]. As a result, the arterioles and venules lying below the capillary loops are never observed.

Efforts have been made to achieve robust imaging of nailfold microvascular structure in its entirety. The ideal technique should be "mesoscopic", i.e. it should be able to able to image at depths of at least 1–1.5 mm in order to reach the whole skin depth, while maintaining resolution of ~5–10 μm in order to be able to image the smallest capillaries and arterioles and venules underlying the epidermis regardless of epidermal thickness [9]. Optical coherence tomography (OCT) fulfills these imaging requirements and has been used by several authors to image the nailfold [11–13]. However, adapting the OCT method to image microvasculature leads to a penetration depth of only ~450 μm and severely reduces axial resolution because of inherent imaging artifacts [149]. These drawbacks, although mitigated somewhat in micro-OCT [15], prevent OCT from providing highly accurate three-dimensional representations of nailfold microvascular structure.

A more powerful alternative may be clinical ultra-wideband raster-scan optoacoustic mesoscopy (UWB-RSOM), a recently developed technique that can resolve the microvascular structure of the skin – including capillaries, arterioles and venules – in label-free mode with a resolution around 10 μm (depending on the implementation) [14,16–18]. UWB-RSOM can reach a penetration depth of 5 mm, while keeping high resolution. Its

* Corresponding author.
E-mail address: v.ntziachristos@tum.de (V. Ntziachristos).
[1] Equal contribution.

https://doi.org/10.1016/j.pacs.2018.02.002

contrast mechanism is based on light absorption. Since hemoglobin is one of the strongest visible light absorbers in tissue, it presents superior capabilities to image the microvasculature in comparison with other label-free mesoscopic techniques like OCT or high-frequency ultrasound imaging [14]. Therefore, in principle, UWB-RSOM may be able to image quantitatively the whole microvascular structure of the nailfold, which would make it superior to current nailfold capillaroscopy methods.

To our knowledge, UWB-RSOM has never been used to image the nailfold microvasculature. It is also unclear whether UWB-RSOM can image the whole microvascular structure under the epidermis. UWB-RSOM using a detector with a central frequency of 100 MHz (UWB-RSOM100; lateral resolution, 18 μm; axial resolution, 4 μm) [14] can image skin capillary loops on top of the dermis, but not in the deeper microvascular plexus. Switching to a detector with a central frequency of 55 MHz (UWB-RSOM55; lateral resolution, 30 μm; axial resolution, 8 μm) can image arterioles and venoules correctly in the mid and deep plexus but not the smallest dermal capillaries directly below the epidermis [19].

We hypothesized that UWB-RSOM55 can resolve morphological parameters of the nailfold capillaries that are of interest for the early diagnosis and prognosis of SSc together with the deeper microvascular structure of the nailfold. To validate our hypothesis, we imaged the nailfold of 6 healthy subjects with a clinical UWB-RSOM55 system and a standard clinical bright-field microscope. We quantified the most relevant parameters of the capillaries used for early diagnosis of SSc with both techniques and compared the obtained values. We show that when the epidermis is too thick for the optical microscope to provide interpretable images, UWB-RSOM55 provides good images. In fact, this system provides the first three-dimensional views of the entire nailfold microvascular structure, opening up new research opportunities on the effects of connective tissue diseases on the microvasculature.

2. Material and methods

2.1. UWB-RSOM system, imaging protocols, image reconstruction and gold standard

In order to test the ability of UWB-RSOM to image microvascular structures in comparison with the gold standard of bright-field microscopy, we examined with six healthy volunteers using both systems. The data acquisition hardware in the UWB-RSOM55 system has been described [14]. The laser wavelength is 532 nm and the repetition rate 500 Hz. The transducer is a custom-made, spherically focused transducer with a central frequency of 50 MHz and bandwidth greater than 100% that can detect frequencies from 10 MHz to 120 MHz. The transducer was scanned over a surface measuring 4 mm x 2 mm, and data were acquired during 70 s (266 × 135 data points).

All participants gave written informed consent to participate in the study, which was approved by the Government of Upper Bavaria. Each volunteer sat in a chair and placed the fourth ("ring") finger of his or her non-dominant hand on a flat surface. Then the UWB-RSOM scan head was placed on top of the finger (Fig. 1a) such that the nailfold region lay within the scanned area (Fig. 1b). An interface unit allows easy placement of the scanner on the targeted skin area. A fast pre-scan is conducted to determine whether the scanned area is near the nailfold or on top of it. Based on the results of this pre-scan, the scanner's position can be changed either through the software or by physically displacing the scanning head in order to target the desired region.

Acquired signals were divided into two frequency bands: 10–40 MHz (low) and 40–120 MHz (high). Signals in the two bands were independently reconstructed using a beam-forming algorithm [14] that generates three-dimensional images. Reconstructions were performed on a cubic grid measuring 4 mm × 2 mm × 1.5 mm,

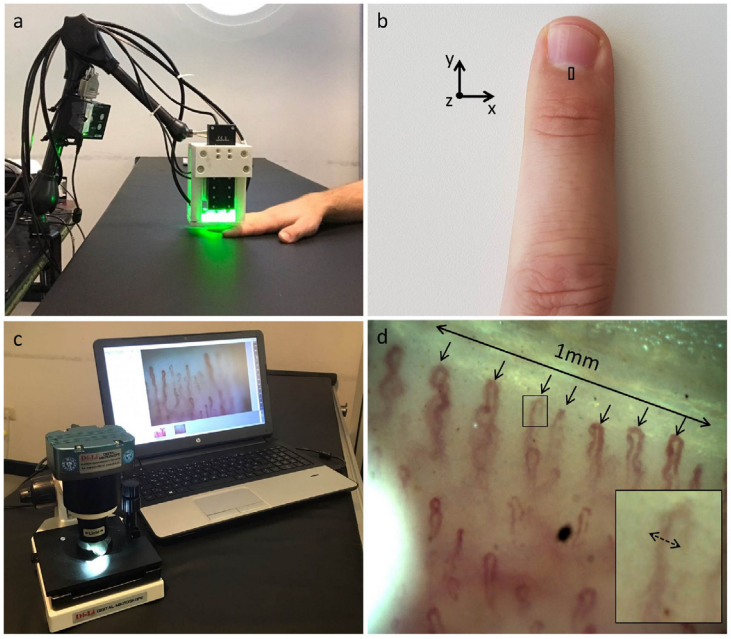

Fig. 1. UWB-RSOM and bright-field microscopy for nailfold capillary analysis. (a) UWB-RSOM system in the process of acquiring data from a nailfold. (b) Fourth (ring) finger of a subject's non-dominant hand, with the RSOM field of view (4 × 2 mm) shown with a black rectangle. The scanned area excludes the nail area, since the large difference in acoustic impedance between the solid nail and the soft underlying tissue distorts the acoustic wavefront used to generate capillary images. (c) Conventional bright-field microscope for nailfold capillaroscopy. (d) Representative nailfold bright-field microscopy image. The density of the capillaries was calculated by counting the number of distal capillaries along a 1-mm length. The maximal capillary diameter was measured as the largest diameter of the erythrocyte column measured from a capillary loops' arterial or venous limb or from the apex of the loop.

where the *x* dimension corresponds to the longitudinal direction of the finger; *y* dimension, to the transverse direction; and *z* dimension, depth (Fig. 1b). Separate reconstruction of frequency bands can reduce noise, especially during reconstruction of high-frequency data [20]. After reconstruction, a composite RGB image was constructed by fusing the low-frequency reconstruction into the red channel, and the high-frequency reconstruction into the green channel. Frequency equalization and motion correction were then applied [14,21].

Immediately after the optoacoustic imaging session, the nailfold of each volunteer was also imaged using a standard clinical bright-field capillaroscope (USB-Kapillarmikroskop Di-Li 2100-A) (Fig. 1c). These results served as the gold standard reference for benchmarking UWB-RSOM.

2.2. Measuring parameters associated to the capillary structure with UWB-RSOM and gold standard

We measured two clinically relevant parameters of nailfold microvascular structure using UWB-RSOM and bright-field capillaroscopy: capillary density and maximal capillary diameter.

2.2.1. Capillary density

Capillary density was determined from bright-field capillaroscopy images as described [8]. A clinician counted the number of capillary loops along a 1-mm line running perpendicular to the longitudinal axis of the finger (Fig. 2d). This procedure allows quantitation of the loops of the capillaries in the row lying closest to the nail, referred to as “distal capillaries”.

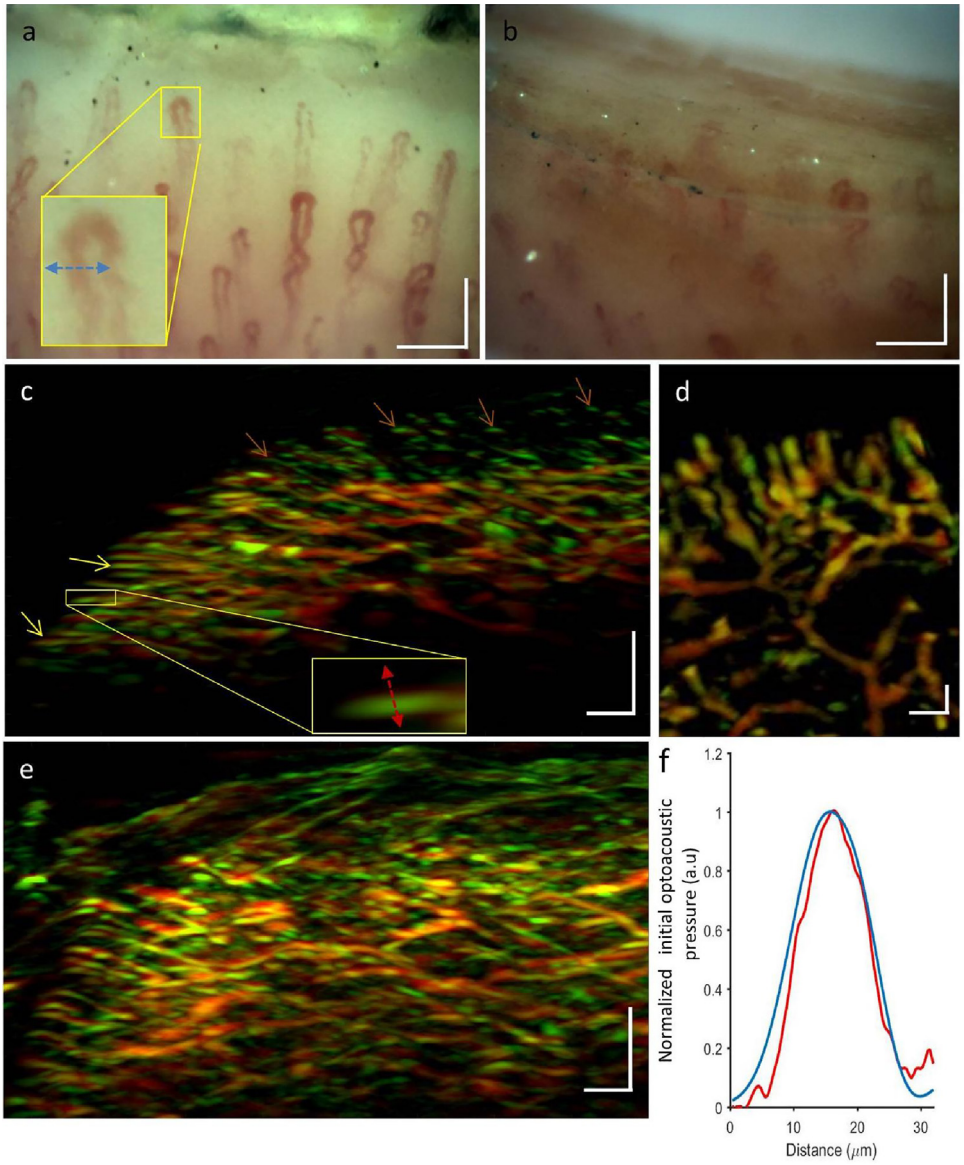

Fig. 2. Comparison of capillary imaging by conventional nailfold capillaroscopy and UWB-RSOM55. (a) Capillaroscopy image of the nailfold of subject 1 with relatively thin, light epidermis. The capillaries can be clearly seen. The yellow box encloses a capillary whose profile (blue line) is displayed in panel (f). (b) Capillaroscopy image of the nailfold of subject 2 with relatively thick, dark epidermis. The capillaries are barely visible and assessment of vascular morphology is difficult. (c) Maximum intensity projection obtained in the sagittal direction by UWB-RSOM55 of a region in close proximity to the region shown in panel (a). Yellow arrows indicate capillaries parallel to the skin, close to the base of the nail. Brown arrows show capillaries far away from the nail that are oriented perpendicular to the skin, such that only their tips are visible. (d) Maximum intensity projection in the coronal direction corresponding to a region in close proximity to the region shown in panel (a). (e) Maximum intensity projection obtained in the sagittal direction by UWB-RSOM55 of a region in close proximity to the region shown in panel (b). (f) Profile of a single capillary in terms of optical signal by nailfold capillaroscopy from panel (a) (blue line) or in terms of optoacoustic signal by UWB-RSOM55 from panel (c) (red line). (For interpretation of the references to colour in thisfigure legend, the reader is referred to the web version of this article.). Scale bars 1: a), b) and d) 150 μm. Scale bars 2: c) and e) 250 μm.

Capillary loop density was measured from UWB-RSOM images by dividing the reconstruction grid into two volumes of 4 mm × 1 mm × 1.5 mm. Capillary density was determined based on 3D images of one of the volumes by a researcher blinded to the bright-field capillaroscopy results.

2.2.2. Capillary diameter

Maximal capillary diameter was determined from six capillary loops for each subject using both imaging techniques. Maximal capillary diameter was calculated from bright-field microscopy images as the largest diameter of the erythrocyte column measured from the arterial or venous limb of a capillary loop or the apex of the loop. A capillary diameter greater than 20 μm is considered to be elevated, and capillaries with diameters greater than 50 μm are defined as "giant" and are associated with development of SSc [2223].

Maximal capillary diameter was calculated from UWB-RSOM images by measuring the area of the capillary loop close to the apex. Profiles were taken in the axial direction, while maximum intensity projections were taken in the sagittal direction. A full-width half-maximum profile perpendicular to the capillary loop was calculated.

3. Results

3.1. Comparison of UWB-RSOM55 with conventional capillaroscopy

Fig. 2a shows a bright-field microscopy image of the finger cuticle belonging to one of the participants in the study (subject 1). The subject has a clear, thin epidermis through which the nailfold capillaries are partially visible, but not capillaries in the deeper dermal plexus. In contrast, Fig. 2b shows a micro-capillaroscopy image of another healthy participant (subject 2), whose epidermis is darker and thicker. Only the tips of the capillaries can be seen, and they are blurry. This is an example of a situation in which conventional nailfold capillaroscopy fails to provide detailed information about capillary morphology.

Fig. 2c depicts the UWB-RSOM55 cross sectional view of the nailfold microvascular structure in subject 1. The smallest capillaries can be seen running parallel to the skin surface towards the nail. Towards the base of the finger, the capillaries gradually orient perpendicularly to the skin surface. Only the tips of these perpendicularly oriented capillaries can be visualized because of the directional nature of the optoacoustic signal [17,24]. The venules and arterioles of the lower plexus can be seen clearly. Fig. 2d shows a coronal view of subject 1, which is reminiscent of the image in Fig. 2a obtained using standard nailfold capillaroscopy. Fig. 2e shows the UWB-RSOM55 cross section of microvasculature in subject 2, indicating that the technique can provide good image quality even when the epidermis is thick and dark. Fig. 2f shows that the profiles of single capillaries were similar for conventional capillaroscopy (red line, lateral profile) and for UWB-RSOM55 (blue line, axial profile. Three-dimensional visualization of the capillary loops (Supplementary Video 1) reveals their arrangement in rows and their orientation towards the nailfold, forming a structure that resembles the spikes of a hedgehog. These results suggest that UWB-RSOM55 can image capillary morphology with comparable performance to conventional nailfold capillaroscopy and can provide interpretable images even when the epidermis is thicker and darker, beyond the capabilities of capillaroscopy.

3.2. Quantification of capillary morphology

Next we wanted to test whether UWB-RSOM is capable of quantifying the density and maximal diameter of capillaries, which clinicians measure in order to detect avascular areas and abnormally large capillaries when diagnosing SSc [1]. Fig. 3 shows that for all subjects, UWB-RSOM55 gave similar estimates as nailfold capillaroscopy. The capillary diameter is consistently 2–3 micrometers bigger in the UWB-RSOM measurements, as expected due to its lower resolution and hence larger point spread function.

4. Discussion

In this paper we have demonstrated that clinical UWB-RSOM55 is capable of imaging the nailfold microvascular structures from the smaller capillaries to larger venules and arterioles, and that it can do so even when the epidermis is relatively thick and dark, when the gold standard of nailfold capillaroscopy fails to provide informative images. We show how UWB-RSOM55 can quantify clinically relevant morphological features of capillaries, giving results similar to those of nailfold capillaroscopy.

This study provides the first quantitative views of complete nailfold microvascular structure, opening up opportunities for basic and clinical research of connective tissue diseases such as SSc [22]. Scleroderma affects not only capillaries but also the rest of the microvascular tree [25], so tools that can image the entire microvascular structure of the nailfold provide highly useful information. For example, when Laser Doppler imaging and thermography, which are sensitive to blood flow in the deep dermis, were combined with microcapillaroscopy, researchers were able to improve the rate of correctly classified disease from 89% to 94% [1]. This highlights the promise of UWB-RSOM55, which offers higher resolution than Laser Doppler or thermographic techniques, especially when imaging deeper vessels, and which provides morphological-structural information, unlike Laser Doppler or thermography.

UWB-RSOM55 may be an alternative to current clinical nailfold capillaroscopy methods, especially when the epidermis around the nail is thick. Further work is needed to verify that the technique is robust to variations in melanin levels in the skin. Preliminary data suggest that the technique has sufficient sensitivity to image deep vessels in individuals ranging from 1 to 5 on the Fitzpatrick scale (Aguirre et al., unpublished).

This is the first time that UWB-RSOM55 has been shown to resolve the smaller capillaries in the skin based on benchmarking with the gold-standard technique of nailfold capillaroscopy. Previous work suggested that UWB-RSOM55 should image the lower dermal micro-vasculature but not the capillary loops.[19] The results in the present study indicate that UWB-RSOM55 can perform better than initially suggested. In fact, the technique provided estimates of capillary density and maximal capillary diameter in good accordance with the gold standard of bright-field capillaroscopy and within the ranges expected for healthy subjects [22]. The discrepancy between the two techniques can be attributed at least in part to the fact that they did not examine identical skin locations, and to the fact that multiple measurements of the same subject show some variability [26]. Nevertheless, the discrepancy between UWB-RSOM55 and bright-field microscopy appears to be relatively small: the standard deviation of the difference in capillary densities measured by the two techniques was 1.09, compared to 1.22 in a previous comparison of two video-based capillaroscopy methods [26].

Like UWB-RSOM55, optoacoustic microscopy can image the capillary loop architecture of the nailfold [27,28]. However, optoacoustic microscopy cannot resolve the entire microvasculature and it is expected to suffer from similar problems as bright-field microcapillaroscopy, since the techniques share the same fundamental resolution limits. Furthermore, UWB-RSOM devices are at the verge of clinical implementation [14] whereas optoacoustic microscopy remains far from the clinic. It is well recognized that scleroderma affects not only the capillaries but also the rest of the

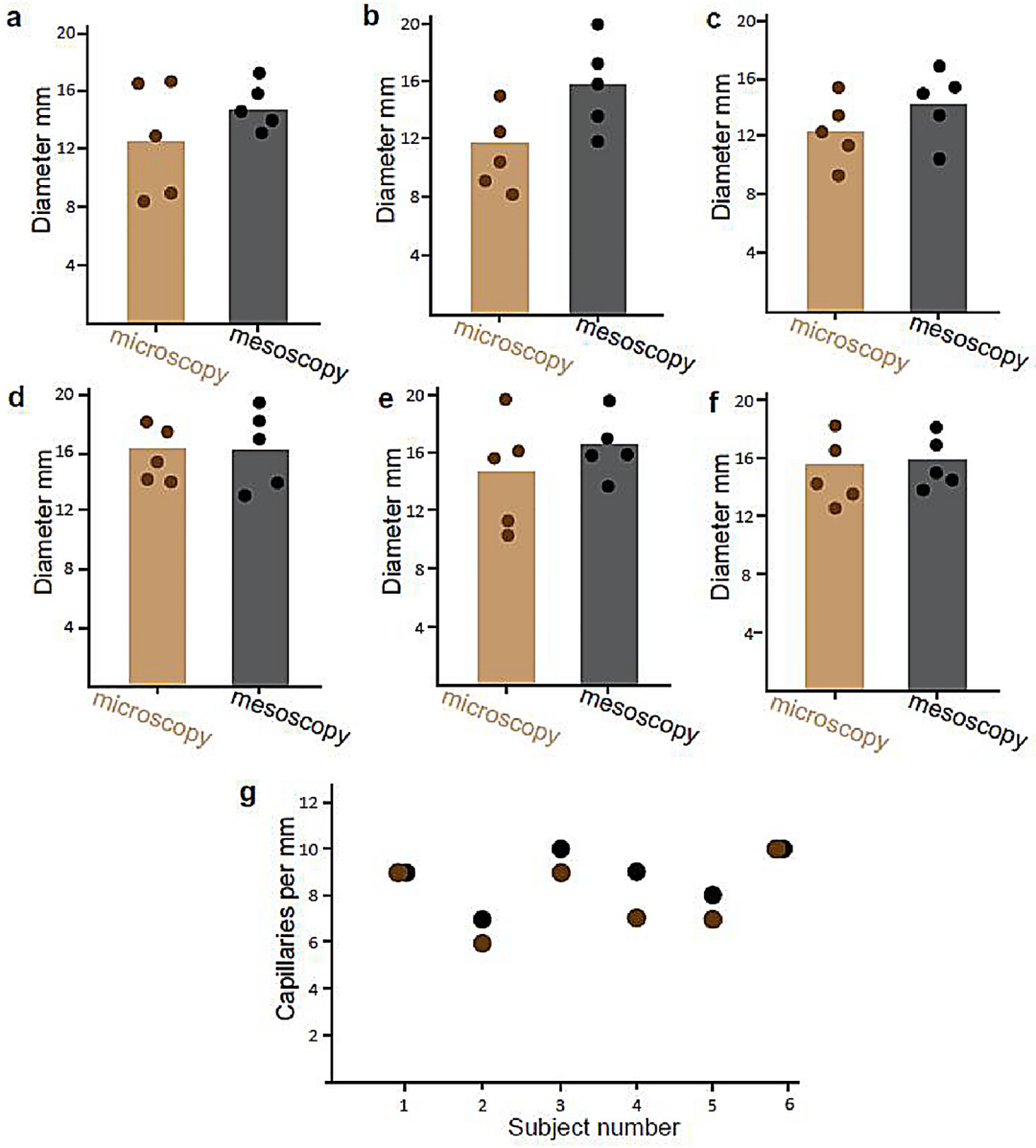

Fig. 3. Comparison of capillary quantitation by conventional nailfold capillaroscopy and UWB-RSOM55. (a–f) Comparison of capillary diameters estimated using capillaroscopy (brown) and UWB-RSOM55 (gray) in 6 healthy subjects. (g) Comparison of capillary diameters estimated using capillaroscopy (brown) and UWB-RSOM55 (gray) in the healthy subjects.

microvascular tree (that is venules and arterioles) [25], therefore it is expected that a tool can image the whole microvascular structure of the nailfold will provide useful information.

One limitation of UWB-RSOM that must be resolved for clinical implementation is the long data acquisition time. The images in the present paper required scanning of approximately 1 min, compared to real time scanning for OCT [29]. Longer scanning time increases the risk of patient motion, which can cause artifacts in the resulting RSOM images. This highlights the need for appropriate motion correction strategies [21].

In this paper we have demonstrated that clinical UWB-RSOM can mimic the ability of bright-field microscopy to characterize capillary parameters relevant for the diagnosis and assessment of SSc, with a penetration depth at least one order of magnitude better. This allows the optoacoustic technique to provide informative images when conventional nailfold capillaroscopy cannot. Therefore UWB-RSOM has a strong potential to become a useful tool for dermatology researchers and clinicians to improve our basic understanding of SSc and its management. Future work should examine the clinical performance of the technique with patients.

Conflict of interest

V. Ntziachristos is a shareholder in iThera-Medical GmBH, Munich, Germany.

Funding

The sponsors did not have any involvement in the study design; collection, analysis and interpretation of data; the writing of the manuscript; the decision to submit the manuscript for publication.

Acknowledgments

This project has received funding from the European Union's Horizon 2020 research and innovation programme under grant agreement no. 687866 (INNODERM) and from the European Research Council (ERC) under the European Union's Horizon 2020 research and innovation programme under grant agreement no. 694968 (PREMSOT).

Appendix A. Supplementary data

Supplementary data associated with this article can be found, in the online version, at https://doi.org/10.1016/j.pacs.2018.02.002.

References

[1] M. Cutolo, A. Sulli, V. Smith, Assessing microvascular changes in systemic sclerosis diagnosis and management, Nat. Rev. Rheumatol. 6 (10) (2010) 578–587.
[2] A. Gabrielli, E.V. Avvedimento, T. Krieg, Scleroderma, N. Engl. J. Med. 360 (19) (2009) 1989–2003.
[3] F.E. Harper, H.R. Maricq, R.E. Turner, R.W. Lidman, E.C. Leroy, A prospective study of Raynaud phenomenon and early connective tissue disease. A five-year report, Am. J. Med. 72 (6) (1982) 883–888.
[4] F. Koenig, M.J. Joyal, A. Fritzler, M. Roussin, G. Abrahamowicz, J.R. Boire, E. Goulet, T. Rich, Y. Grodzicky, J.L. Raymond, Autoantibodies and microvascular damage are independent predictive factors for the progression of Raynaud's phenomenon to systemic sclerosis: a twenty-year prospective study of 586 patients, with validation of proposed criteria for early systemic sclerosis, Arthritis Rheum. 58 (12) (2008) 3902–3912.
[5] A.B. Maricq, E.C. Weinberger, Early detection of scleroderma-spectrum disorders by in vivo capillary microscopy: a prospective study of patients with Raynaud's phenomenon, J. Rheumatol. 9 (2) (1982) 289–291.
[6] F. van den Hoogen, D. Khanna, J. Fransen, S.R. Johnson, M. Baron, A. Tyndall, M. Matucci-Cerinic, R.P. Naden, T.A. Medsger, P.E. Carreira Jr., G. Riemekasten, P.J. Clements, C.P. Denton, O. Distler, Y. Allanore, D.E. Furst, A. Gabrielli, M.D. Mayes, J.M. van Laar, J.R. Seibold, L. Czirjak, V.D. Steen, M. Inanc, O. Kowal-Bielecka, U. Muller-Ladner, G. Valentini, D.J. Veale, M.C. Vonk, U.A. Walker, L. Chung, D.H. Collier, M. Ellen Csuka, B.J. Fessler, S. Guiducci, A. Herrick, V.M. Hsu, S. Jimenez, B. Kahaleh, P.A. Merkel, S. Sierakowski, R.M. Silver, R.W. Simms, J. Varga, J.E. Pope, Classification criteria for systemic sclerosis: an American college of rheumatology/European league against rheumatism collaborative initiative, Ann. Rheum. Dis. 72 (11) (2013) 1747–1755.
[7] M.Y. Shenavandeh, M.A. Haghighi, Nailfold digital capillaroscopic findings in patients with diffuse and limited cutaneous systemic sclerosis, Reumatologia 55 (1) (2017) 15–23.
[8] H.M. Hofstee, E.H. Serne, C. Roberts, R. Hesselstrand, A. Scheja, T.L. Moore, M. Wildt, J.B. Manning, A. Vonk Noordegraaf, A.E. Voskuyl, A.L. Herrick, A multicentre study on the reliability of qualitative and quantitative nail-fold videocapillaroscopy assessment, Rheumatology (Oxford) 51 (4) (2012) 749–755.
[9] V. Ntziachristos, Going deeper than microscopy: the optical imaging frontier in biology, Nat. Methods 7 (8) (2010) 603–614.
[11] H.C. Ring, L. Themstrup, C.A. Banzhaf, G.B. Jemec, M. Mogensen, Dynamic optical coherence tomography capillaroscopy: a new imaging tool in autoimmune connective tissue disease, JAMA Dermatol. 152 (10) (2016).
[12] K.K. Lee, A. Mariampillai, J.X. Yu, D.W. Cadotte, B.C. Wilson, B.A. Standish, V.X. Yang, Real-time speckle variance swept-source optical coherence tomography using a graphics processing unit, Biomed. Opt. Exp. 3 (7) (2012) 1557–1564.
[13] H.M. Subhash, M.J. Leahy, Microcirculation imaging based on full-range high-speed spectral domain correlation mapping optical coherence tomography, J. Biomed. Opt. 19 (2) (2014) 21103.
[14] J. Aguirre, M. Schwarz, N. Garzorz, M. Omar, A. Buehler, K. Eyerich, V. Ntziachristos, Precision assessment of label-free psoriasis biomarkers with ultra-broadband optoacoustic mesoscopy, Nat. Biomed. Eng. 1 (2017) 0068.
[15] W.J. Choi, R.K. Wang, Volumetric cutaneous microangiography of human skin in vivo by VCSEL swept-source optical coherence tomography, Quantum Elec. (Woodbury) 44 (8) (2014) 740.
[16] M. Omar, J. Gateau, V. Ntziachristos, Raster-scan optoacoustic mesoscopy in the 25–125 MHz range, Opt. Lett. 38 (14) (2013) 2472–2474.
[17] J. Aguirre, M. Schwarz, D. Soliman, A. Buehler, M. Omar, V. Ntziachristos, Broadband mesoscopic optoacoustic tomography reveals skin layers, Opt. Lett. 39 (21) (2014) 6297.
[18] M. Schwarz, M. Omar, A. Buehler, J. Aguirre, V. Ntziachristos, Implications of ultrasound frequency in optoacoustic mesoscopy of the skin, IEEE Trans. Med. Imaging 34 (2) (2015) 672–677.
[19] M. Schwarz, D. Soliman, M. Omar, A. Buehler, S.V. Ovsepian, J. Aguirre, V. Ntziachristos, Optoacoustic dermoscopy of the human skin: tuning excitation energy for optimal detection bandwidth with fast and deep imaging in vivo, IEEE Trans. Med. Imaging 36 (6) (2017) 1287–1296.
[20] M. Omar, M. Schwarz, D. Soliman, P. Symvoulidis, V. Ntziachristos, Pushing the optical imaging limits of cancer with multi-Frequency-Band raster-Scan optoacoustic mesoscopy (RSOM), Neoplasia 17 (2) (2015) 208–214.
[21] M. Schwarz, N. Garzorz-Stark, K. Eyerich, J. Aguirre, V. Ntziachristos, Motion correction in optoacoustic mesoscopy, Sci. Rep. 7 (1) (2017) 10386.
[22] A.C. Trombetta, V. Smith, C. Pizzorni, M. Meroni, S. Paolino, C. Cariti, B. Ruaro, A. Sulli, M. Cutolo, Quantitative alterations of capillary diameter have a predictive value for development of the capillaroscopic systemic sclerosis pattern, J. Rheumatol. 43 (3) (2016) 599–606.
[23] W. Grassi, P.D. Medico, F. Izzo, C. Cervini, Microvascular involvement in systemic sclerosis: capillaroscopic findings, Semin. Arthritis Rheum. 30 (6) (2001) 397–402.
[24] T. Gateau, O. Chaigne, S. Katz, E. Gigan, Improving visibility in photoacoustic imaging using dynamic speckle illumination, arXiv preprint arXiv 1308.0243 (2013).
[25] M. Manetti, S. Guiducci, L. Ibba-Manneschi, M. Matucci-Cerinic, Mechanisms in the loss of capillaries in systemic sclerosis: angiogenesis versus vasculogenesis, J. Cell. Mol. Med. 4 (6a) (2010) 1241–1254.
[26] F. Ingegnoli, R. Gualtierotti, C. Lubatti, C. Bertolazzi, M. Gutierrez, P. Boracchi, M. Fornili, R. De Angelis, Nailfold capillary patterns in healthy subjects: a real issue in capillaroscopy, Microvasc. Res. 90 (2013) 90–95.
[27] L. Lin, P. Zhang, S. Xu, J. Shi, L. Li, J. Yao, L. Wang, J. Zou, L.V. Wang, Handheld optical-resolution photoacoustic microscopy, J. Biomed. Opt. 22 (4) (2017) 41002.
[28] S. Hu, L.V. Wang, Optical-resolution photoacoustic microscopy: auscultation of biological systems at the cellular level, Biophys. J. 105 (4) (2013) 841–847.
[29] M. Mogensen, L. Thrane, T.M. Jorgensen, P.E. Andersen, G.B. Jemec, OCT imaging of skin cancer and other dermatological diseases, J. Biophotonics 2 (6–7) (2009) 442–451.

Juan Aguirre Dr. Juan Aguirre received his M.Sc. degree in Physics from Autonomous University of Madrid in 2007 and his M.Sc. degree in Mathematical Engineering from the Complutense University of Madrid in 2011. From 2007 to 2012 he pursued his Ph.D title in the Laboratory for Molecular Imaging of the Gregorio Maranion Hospital in Madrid, doing short stays at Foundation for Research and Technology in Greece and the University of Pennsylvania in the EEUU. After obtaining his ph.D he joined the Institute of Biological and Medical Imaging (IBMI) at the Helmholtz Zentrum München with an indivudial Marie Curie Scholarship from the EU. He is currently a Junior Group Leader at IBMI. His research interests include developing and applying Optoacoustic Imaging techniques to solve unmet clinical needs.

Benedikt Hindelang Benedikt Hindelang recieved his medical degree from Technical University Munich (TUM) School of Medicine in 2015 and submitted his doctoral thesis (Dr. med.) to the, Institute of Occupational, Social and Environmental Medicine" of Ludwig-Maximilians-Universitaet Munich in 2016. Afterwards he joined the Department of Dermatology and Allergology of TUM's university hospital and is employed as a postdoctoral fellow at TUM Chair for Biological Imaging. His research interests include the application of optocoustic imaging to unmet clinical needs in dermatology.

A. Bereznhoi Andrei Bereznhoi obtained his bachelor degree in Technical Physics in 2011 from the St.Petersburg Polytechnic University. He obtained his master degree also in TechnicalPhysics from the St. Petersburg Polytechnic in 2013. He is currently a PhDcandidate in the Institute for Biological and Medical Imaging in Munich. His researchinterest comprise medical imaging with a focus on photoacoustic technics.

Ulf Darsow Professor Darsow (b. 1965) studied medicine at the University of Düsseldorf and worked in dermatology and allergy at the university hospitals of Hamburg and TU Munich. As a postdoctoral researcher he worked in the Dept. of Neurophysiology of University Hospital Eppendorf. At TUM, he is senior physician in the Dermatology Dept. with research areas clinical and experimental allergy, imaging and pruritus perception, and development of diagnostic tools. Professor Darsow received numerous awards for research in these areas e.g. from the German Society for Allergy and Clinical Immunology.

Felix Lauffer Dr. Felix Lauffer finished his studies of medicine in 2013 and received his MD degree from the Technical University of Munich for his research about t cell subtypes in autoimmune pancreatitis at the Department of General Surgery. In 2014 he started working at the Department of Dermatology and Allergy at the Technical University of Munich and is currently finishing his PhD about autoimmune and chronic inflammatory skin reaction patterns and his specialist training in dermatology and venerology.

Kilian Eyerich The research area of Professor Eyerich (b. 1979) is the immunology of inflammatory skin diseases such as psoriasis or atopic eczema. As an MD/PhD, his ultimate goal is to improve patient care through the development of innovative diagnostic and therapeutic tools. Professor Eyerich studied medicine at the University of Würzburg and at TUM. After graduation he joined TUM's "Medical Life Science and Technology" PhD programme. He also worked as a postdoctoral researcher at the Istituto Dermopatico Dell'immacolata in Rome. Professor Eyerich has received numerous grants and awards for his translational research activities. These have been from organizations such as the Bavarian Academy of Sciences and Humanities, the German Research Foundation, the Fritz Thyssen Foundation and the Bavarian Research Foundation. In 2013 he was awarded a Heisenberg Professorship by the German Research Foundation.

Tilo Biedermann The research of Professor Biedermann focuses on the biology of the skin, immunology and allergology. His research deals with the regulation of tolerance-promoting and inflammatory immune responses. His research activities range from basic research to translating his findings into clinical applications. Professor Biedermann studied medicine at LMU Munich where he also completed his training leading to German medical board certification in dermatology and allergology. During this time he joined the immunology research group of Professor Röcken. As a recipient of a DFG grant he then went to Vienna where he acquired his postdoctoral teaching qualification(habilitation) in 2001. In 2003 he was appointed to a C3 professorship position in the Department of Dermatology at the University Hospital of Tübingen where he stayed until 2014. He has held posts as a senior physician in the fields of allergology, allergological and immunological laboratory diagnostics and in a allergology and immunology research group.

Vasilis Ntziachristos Professor Vasilis Ntziachristos received his PhD in electrical engineering from the University of Pennsylvania, USA, followed by a postdoctoral position at the Center for Molecular Imaging Research at Harvard Medical School. Afterwards, he became an Instructor and following an Assistant Professor and Director at the Laboratory for Bio-Optics and Molecular Imaging at Harvard University and Massachusetts General Hospital, Boston, USA. Currently, he is the Director of the Institute for Biological and Medical Imaging at the Helmholtz Zentrum in Munich, Germany, as well as a Professor of Electrical Engineering, Professor of Medicine and Chair for Biological Imaging at the Technical University Munich. His work focuses on novel innovative optical and optoacoustic imaging modalities for studying biological processes and diseases as well as the translation of these findings into the clinic.